

## Supporting Information

### Experimental Section

#### Synthesis of $\text{Bi}_{19}\text{S}_{27}\text{Cl}_3$ (BSC)

788.8 mg  $\text{BiCl}_3$  (2.5 mmol), 243.6 mg thiourea (3.2 mmol), and 0.1 g EDTA were added to 35 mL ethanol. The mixture was vigorously stirred at room temperature for one hour. The pale yellow dispersion was transferred into a 50 mL PTFE-lined autoclave, sealed, and heated at 180°C for 72 hours. Following reaction completion, the autoclave was cooled to room temperature. The resulting black slurry was removed, and the precipitate was thoroughly washed with water and ethanol to remove unreacted components. The black solid was dried overnight in a vacuum oven at 80°C. BSC nanorods were ultimately obtained as a black powder.

#### Synthesis of x-Mn-BSC

50 mg Mn-based ionic liquid, 788.8 mg  $\text{BiCl}_3$  (2.5 mmol), 243.6 mg thiourea (3.2 mmol), and 0.1 g EDTA were added to 35 mL ethanol. The mixture was vigorously stirred at room temperature for one hour. The pale yellow dispersion was transferred into a 50 mL PTFE-lined autoclave, sealed, and heated at 180°C for 72 hours. Following reaction completion, the autoclave was cooled to room temperature. The resulting black slurry was removed, and the precipitate was thoroughly washed with water and ethanol to remove unreacted components. The black solid was dried overnight in a vacuum oven at 80°C. The black powder obtained is 5-Mn-BSC. By adjusting the Mn-based ionic liquid content to 30 and 70 mg, the resulting samples were designated 3-Mn-BSC and 7-Mn-BSC respectively. As 5-Mn-BSC exhibited the most favourable photocatalytic performance, all instances of Mn-BSC referenced herein denote 5-Mn-BSC.

### Characterizations

The morphology and local atomic structure were determined using transmission electron microscopy (TEM, JEOL-2100F) and aberration-corrected high-angular annular dark field scanning transmission electron microscopy operated at 80 kV (HAADF-STEM, JEM-ARM200F). X-ray diffraction patterns were collected on D8ADVANCE by monochromatic Cu K $\alpha$  irradiation. Fourier-transform infrared (FTIR) spectroscopy was detected on a Nicolet 380 (American). X-ray photoelectron spectroscopy (XPS) was measured on Kratos AXIS Supra XPS with monochromatic Al-K $\alpha$  radiation as X-ray source for excitation. UV-vis diffuse reflectance spectra (DRS) were obtained by UV-3600 spectrophotometer (Tokyo, Japan). The nuclear magnetic resonance is tested using AVANCE NEO 500MHz. Ultrafast transient absorption (TA) spectra were collected over a femtosecond laser amplifier system (Spitfire Ace, Spectra Physics). The output beam was split into two beams. One was used to generate 750 nm pump light, and the other beam was focused into a sapphire plate, generating a broadband white light continuum probe beam. To test the Zeta potential, the sample was tested on the Malvern Zetasizer Nano-S90 (England) and the suspensions of each material in aqueous solution media (0.1 mg mL<sup>-1</sup>) were prepared and measured separately. The TS-SPV signal was recorded by using a 500 MHz digital phosphor oscilloscope (TDS 5054, Tektronix). The specific surface areas of the as-prepared samples were measured by nitrogen adsorption-desorption isotherms on the Micrometrics ASAP 2020 system, employing a fitting analysis based on the Brunauer-Emmett-Teller (BET) equation.

### **Experiment on Photoelectrochemical**

The electrochemical analysis was carried out on a CHI760E electrochemical analyzer using a three-electrode photoelectrochemical cell device, with Ag/AgCl (saturated KCl), Pt wire and the prepared sample membrane as the reference, counter and working electrodes, respectively. 5 mg of catalyst sample was dispersed in a mixed solution of 600  $\mu$ L ethanol and 40  $\mu$ L naphthol, and the suspension was obtained by ultrasonic dispersion. The working electrode was then prepared by dropping 100  $\mu$ L of the suspension onto FTO glass. The unbiased photocurrent response curve was

measured under simulated visible light with a controlled light intensity of 100 mW/cm<sup>2</sup> using 0.5 M Na<sub>2</sub>SO<sub>4</sub> aqueous solution as electrolyte. Electrochemical impedance spectroscopy (EIS) measurements were carried out at open-circuit potentials with an applied AC voltage of amplitude 10 mV at 0 V in the absence of light and Ag/AgCl in the frequency range of 100 kHz to 0.1 Hz. In order to determine the semiconductor type and flat-carrying potential of the material, Mott-Schottky (MS) plots were recorded at an AC frequency of 1000 Hz.

### **Photocatalytic NO<sub>3</sub><sup>-</sup> to NH<sub>4</sub><sup>+</sup> synthesis**

The 10 mg photocatalyst was added to the mixed solution of 10 ml ethylene glycol and 100 ml 0.16 mmol L<sup>-1</sup> nitrate, and then added to the quartz photocatalytic reactor after full ultrasonic dissolution. The experiment is performed under the condition of continuous stirring and constant temperature water bath of 25 °C. A 300 W Xenon lamp with different cut-off filters is employed as light source, such as 320-780 nm for UV-vis irradiation, >800 nm for NIR irradiation. Every 20 minutes, 3 mL test solution was collected. The generated NH<sub>3</sub> is detected by ion chromatography (930 compact IC Flex, Metrohm) and Nessler's reagent.

### **In-situ FTIR measurements**

In situ Fourier transform infrared (FTIR) spectra were collected on a Thermo Fisher Scientific Nicolet iZ10 spectrometer. The catalyst sample was placed in the reaction cell and saturated with a mixed solution of ethylene glycol and nitrate ions (1:10 by volume) to mimic the actual reaction environment. After allowing the system to reach adsorption-desorption equilibrium in the dark for 30 minutes, the xenon lamp was switched on to initiate the photoreaction. Spectral data were then recorded at 5-minute intervals to monitor the dynamic evolution of reaction intermediates.

### **NH<sub>3</sub> TPD**

Weigh 100 mg of samples in the reaction tube, and then increase the temperature from room temperature to 300 °C at 10 °C/min for drying pretreatment, purge by He air

flow (30 mL/min) for 1h, cool down to 50 °C (or 100 °C), pass 7% NH<sub>3</sub>/He mixture (30 mL/min) for 30 min until saturated, and then switch to He air flow (30 mL/min) for 60min to remove the weakly adsorbed NH<sub>3</sub> on the surface, and finally desorb by TCD under He atmosphere at 10 °C/min to 600 °C. The weakly physically adsorbed NH<sub>3</sub> on the surface was removed for 60 min, and finally the adsorption was carried out under He atmosphere at a temperature increase rate of 10 °C/min up to 600 °C, and the removed gases were detected by TCD.

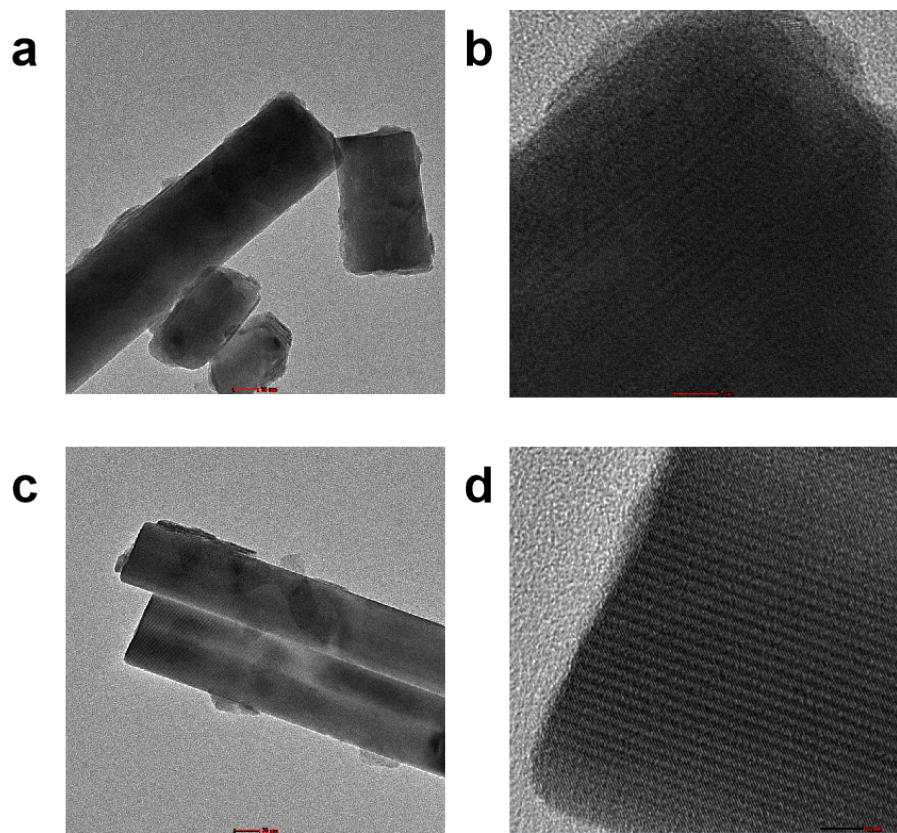


**Fig. S1** TEM images of (a, b) BSC and (c, d) Mn-BSC.

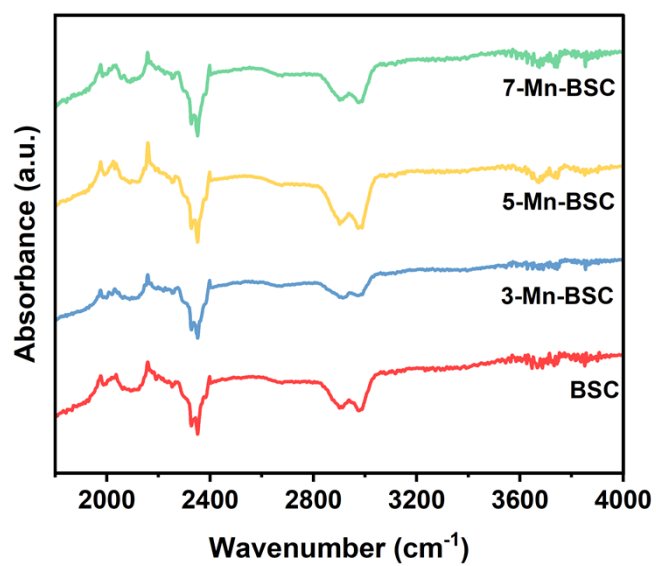


**Fig. S2** FTIR images of BSC, 3-Mn-BSC, 5-Mn-BSC and 7-Mn-BSC.

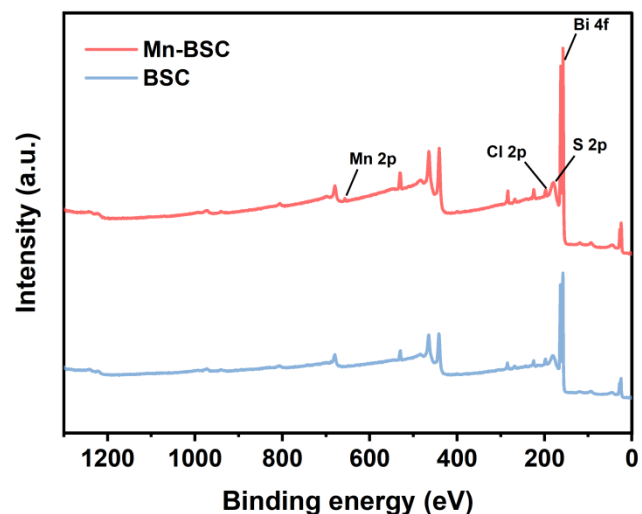


**Fig. S3** X-ray photoelectron spectra survey.

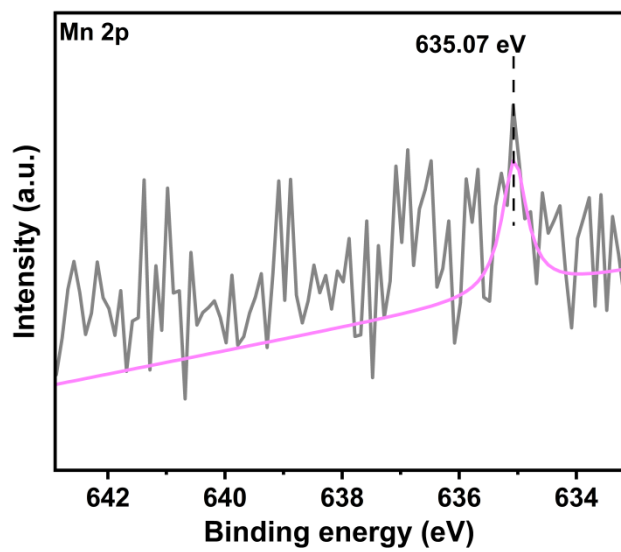


**Fig. S4** XPS spectra of Mn 2p.

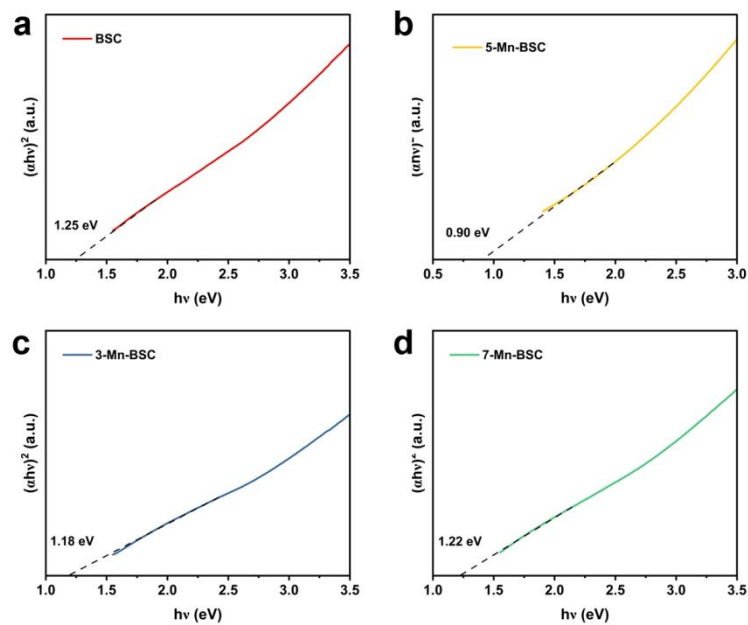


**Fig. S5** Tauc plot of (a) BSC, (b) 5-Mn-BSC, (c) 3-Mn-BSC and (d) 7-Mn-BSC.

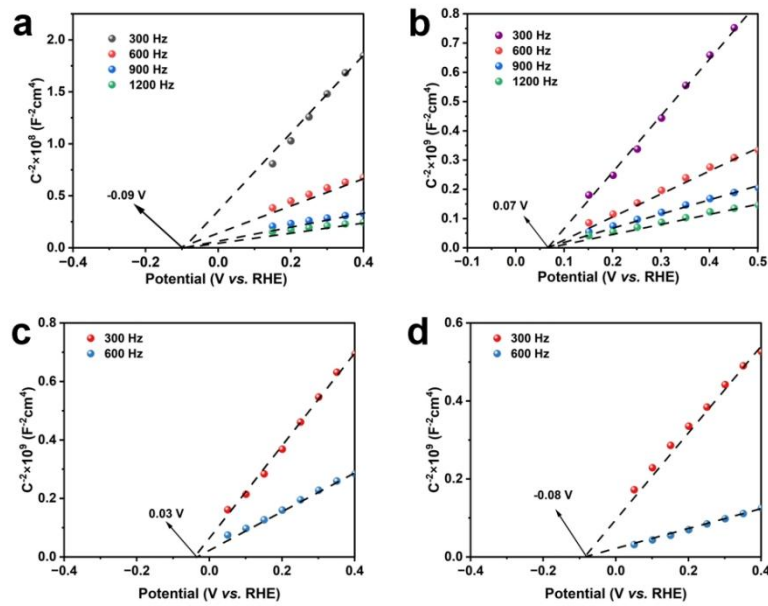


**Fig. S6** Mott-Schottky plots of (a) BSC, (b) 5-Mn-BSC, (c) 3-Mn-BSC and (d) 7-Mn-BSC.

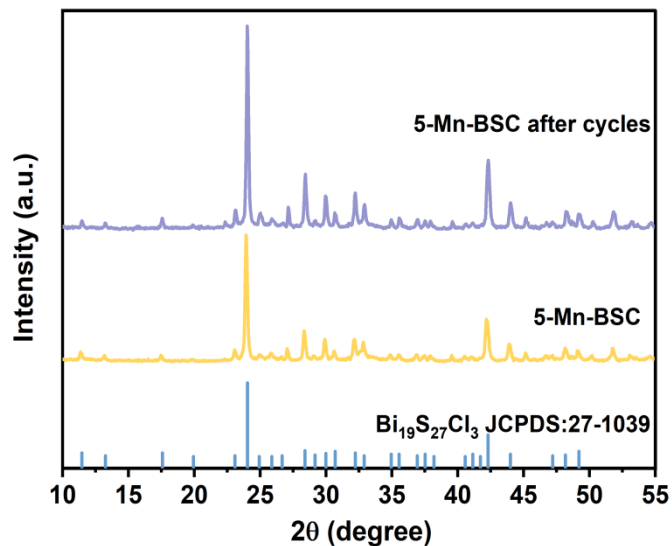


**Fig. S7** XRD result of 5-Mn-BSC after 5 cycles.

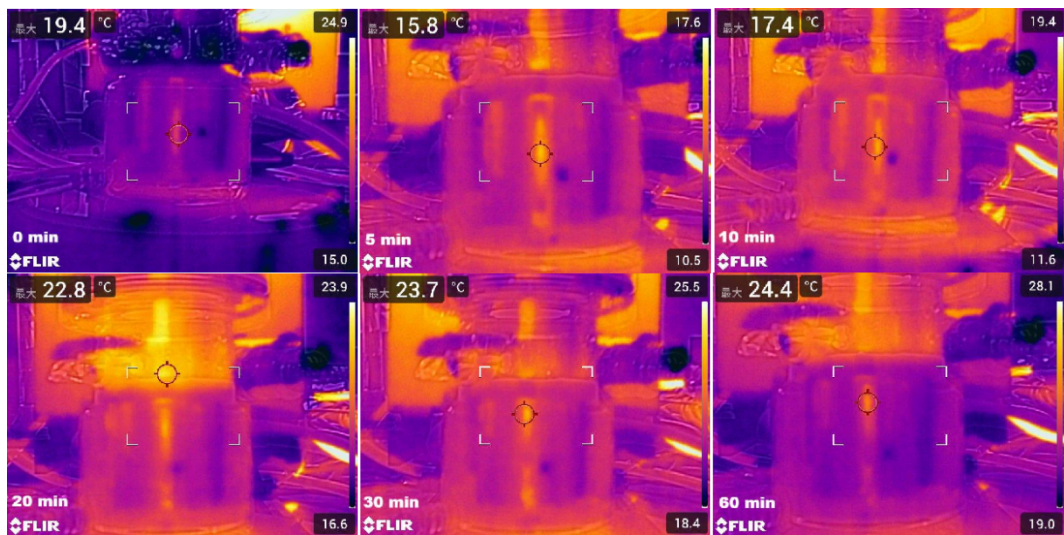


**Fig. S8** Timeline combined with photothermal mapping images of Mn-BSC during photocatalytic reactions ( $\lambda > 800$  nm).

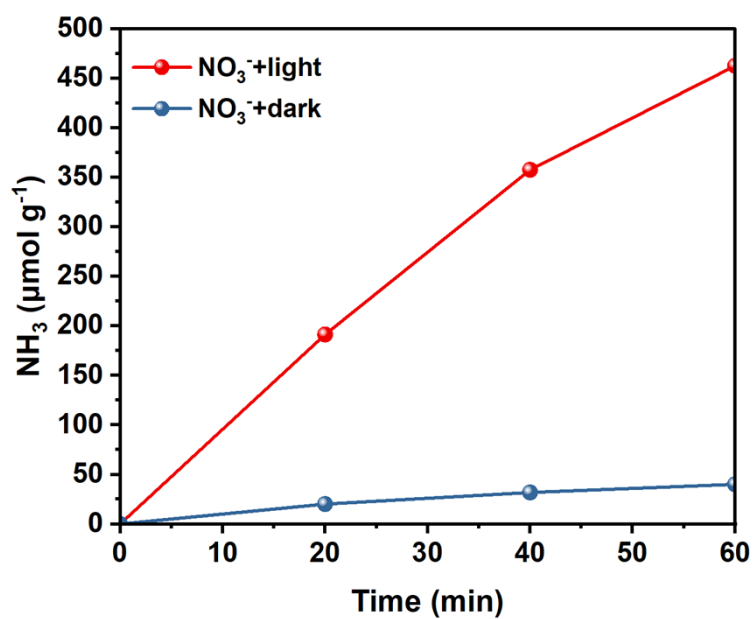


**Fig. S9** 5-Mn-BSC catalyst for nitrate reduction reaction under dark conditions.

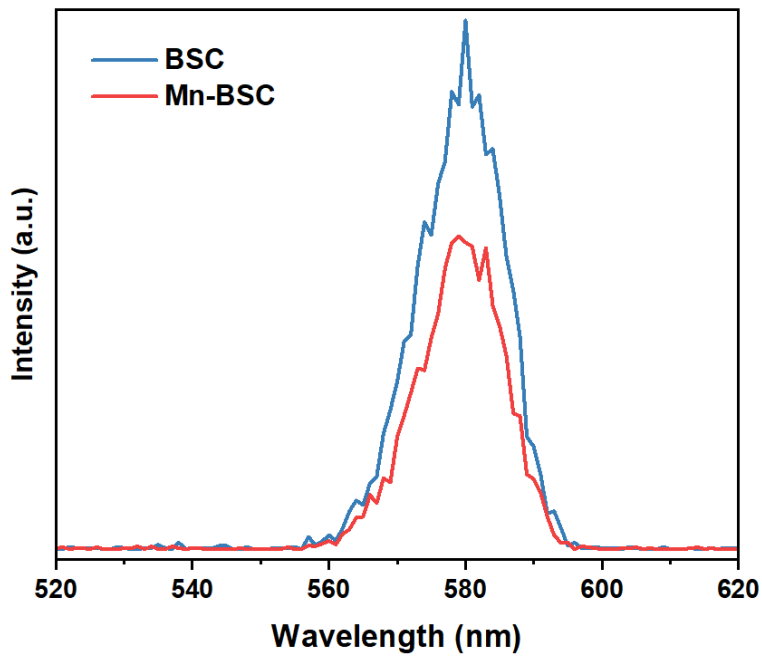


**Fig. S10** Steady-state photoluminescence (PL) spectroscopy of BSC and Mn-BSC.

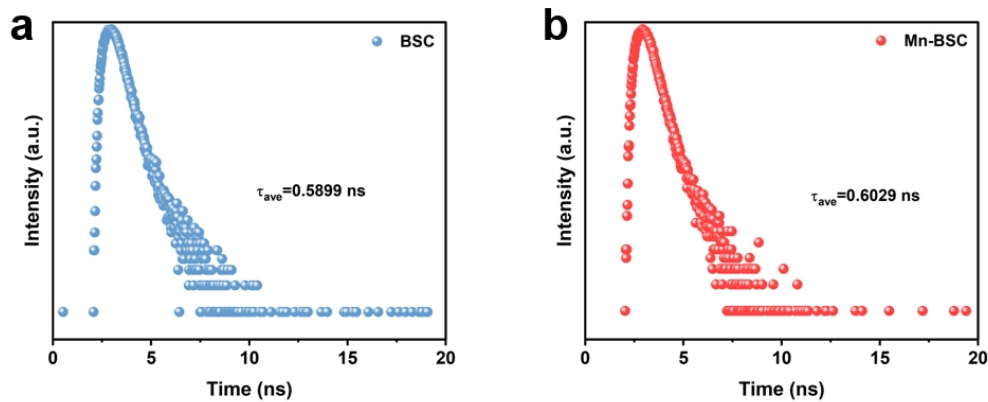


**Fig. S11** Time-resolved photoluminescence spectroscopy (TRPL) spectra of (a) BSC and (b) Mn-BSC.

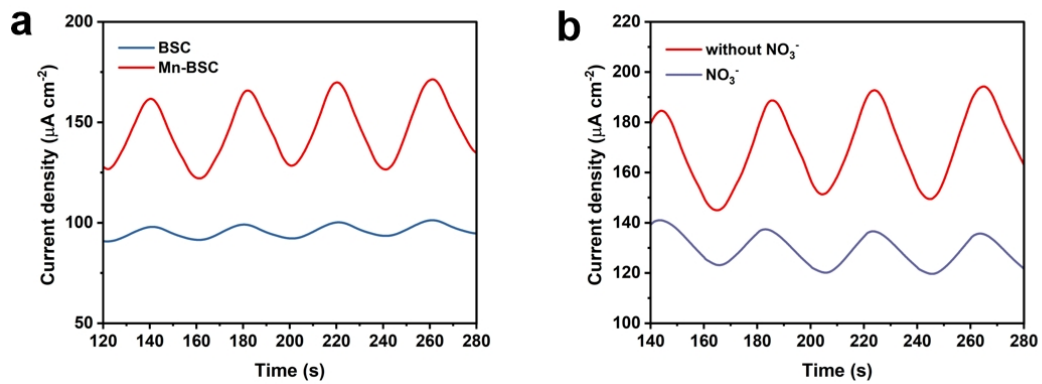


**Fig. S12** (a) Transient photocurrent density of BSC and Mn-BSC. (b) Transient photocurrent density with  $\text{NO}_3^-$  of Mn-BSC.

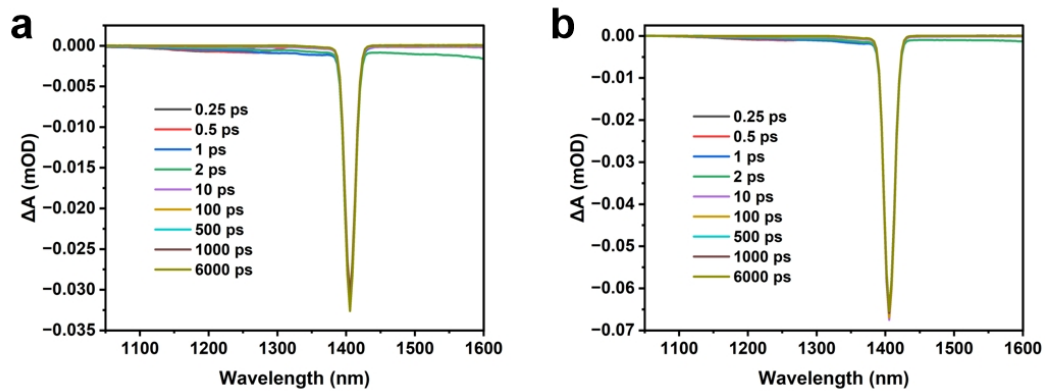


**Fig. S13** Transient absorption spectra of (a) BSC and (b) Mn-BSC.

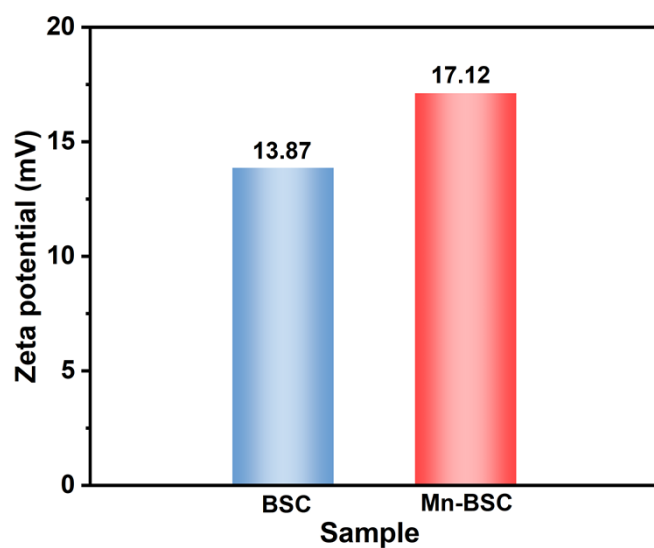


**Fig. S14** Zeta potential of BSC and Mn-BSC.

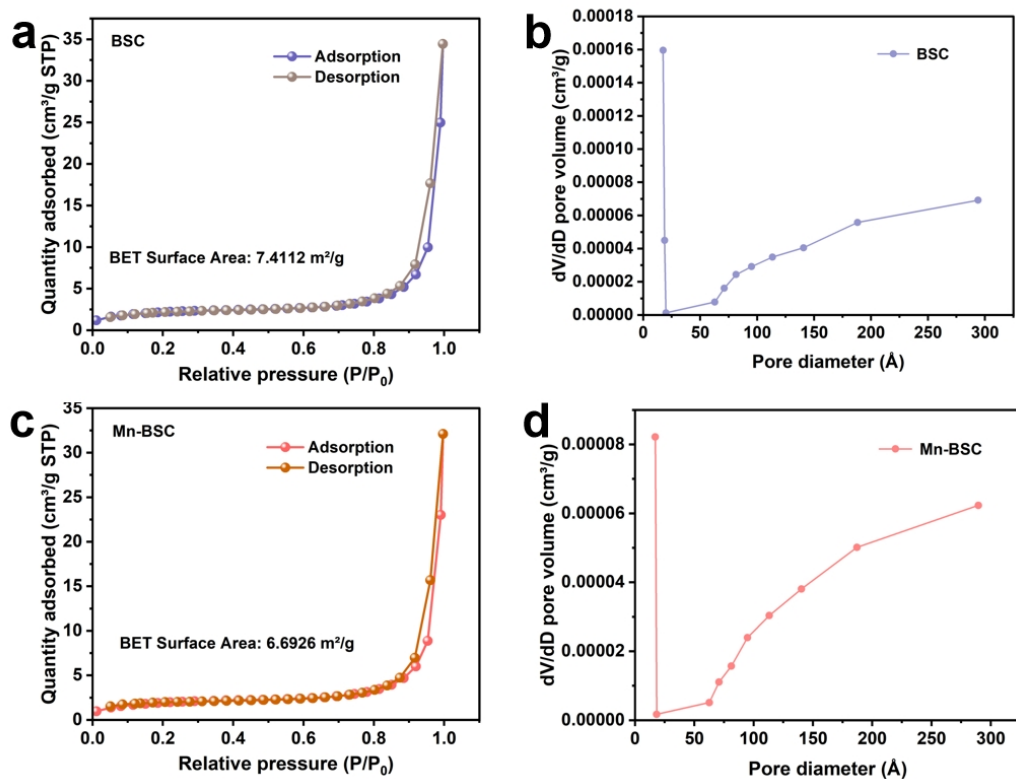


**Fig. S15** Nitrogen adsorption-desorption isotherms of (a) BSC and (c) Mn-BSC. Pore size distribution of (b) BSC and (d) Mn-BSC.

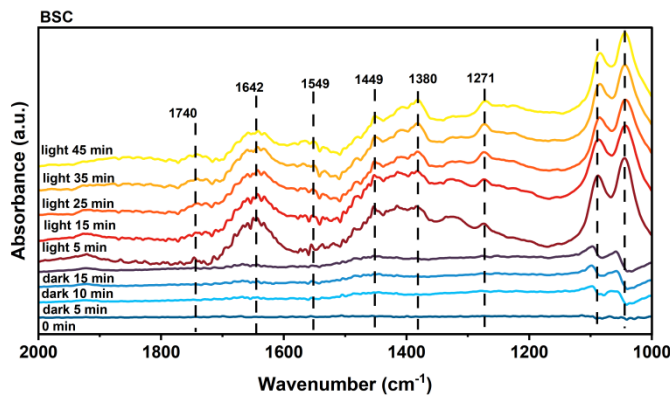


**Fig. S16** In-situ FTIR spectra of BSC for  $\text{NO}_3^-$ RR.

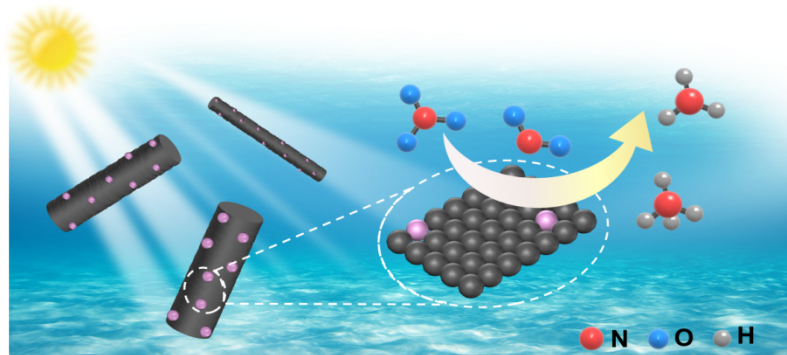


**Fig. S17** Schematic diagram of Mn-BSC photocatalytic ammonia synthesis.

**Table S1.** Comparison of  $\text{NH}_3$  generation performance of different catalysts.

| Photocatalyst | Conditions   | Ammonia synthesis rate                      | References |
|---------------|--|---|------------|
| Mn-BSC        | 300 W Xe lamp, 320-780 nm UV-vis irradiation, 1 mg catalyst, 100 mL $\text{KNO}_3$ 10 mg $\text{L}^{-1}$ solution, 10 mL ethylene glycol | 1276.1 $\mu\text{mol g}^{-1} \text{h}^{-1}$ | This work  |

|   |   |   |  |
|---|---|---|--|
| Mn-BSC  | 300 W Xe lamp, >800 nm for NIR irradiation, 10 mg catalyst, 100 mL $\text{KNO}_3$ 10 mg $\text{L}^{-1}$ solution, 10 mL ethylene glycol   | 138.6 $\mu\text{mol g}^{-1} \text{h}^{-1}$  | This work                                  |
| Mn-BSC  | 300 W Xe lamp, 320-780 nm UV-vis irradiation, 10 mg catalyst, 100 mL $\text{KNO}_2$ 10 mg $\text{L}^{-1}$ solution, 10 mL ethylene glycol | 2150.2 $\mu\text{mol g}^{-1} \text{h}^{-1}$ | This work                                  |
| Ni- $\text{W}_{18}\text{O}_{49}$                                      | 300 W Xe lamp, 10 mg catalyst, 100 mL $\text{KNO}_3$ solution (10 mg $\text{L}^{-1}$ ), 10 mL ethylene glycol                             | 688 $\mu\text{mol g}^{-1} \text{h}^{-1}$    | Appl. Catal. B Environ, 2026, 382, 125987. |
| AgCu-CN   | 300 W Xe lamp, $\geq$ 420 nm, 20 mg catalyst, 100 mL 20 mg $\text{L}^{-1}$ $\text{NO}_3^-$ , 10 mL ethylene glycol                        | 630.5 $\mu\text{mol g}^{-1} \text{h}^{-1}$  | Angew. Chem. Int. Ed. 2025, 11, e202516964 |
| Fe-CuInS <sub>2</sub>   | 300 W Xe lamp, 320-780 nm UV-vis irradiation, 10 mg catalyst, 100 mL 10 mg $\text{L}^{-1}$ $\text{NO}_3^-$ , 10 mL ethylene glycol        | 455 $\mu\text{mol g}^{-1} \text{h}^{-1}$    | Mater. Today, 2025, 86, 96-103.            |
| Defect-rich CaIn <sub>2</sub> S <sub>4</sub>                          | 300 W Xe lamp, 10 mg catalyst, 100 mL 10 mg $\text{L}^{-1}$ $\text{NO}_3^-$ , 10 mL ethylene glycol                                       | 406 $\mu\text{mol g}^{-1} \text{h}^{-1}$    | Small, 2024, 20, 2402808.                  |
| Mn <sub>x</sub> In <sub>2</sub> S <sub>y</sub>                        | 300 W Xe lamp, 320-780 nm UV-vis irradiation, 10 mg catalyst, 100 mL 10 mg $\text{L}^{-1}$ $\text{NO}_3^-$ , 10 mL ethylene glycol        | 515.8 $\mu\text{mol g}^{-1} \text{h}^{-1}$  | ACS Nano, 2024, 18, 21585-21592.           |
| Au <sub>2</sub> -COF  | The AM1.5 filter is installed on the Xenon lamp, 5 mg catalyst, 100 mL 10 mg $\text{L}^{-1}$ $\text{NaNO}_3$                              | 382.48 $\mu\text{mol g}^{-1} \text{h}^{-1}$ | Chin. J. Catal., 2025, 73, 358-367         |
| MoS <sub>2-x</sub> /ZnIn <sub>2</sub> S <sub>4-x</sub> heterojunction | 300 W Xenon lamp, $\geq$ 420 nm, 20 mg catalyst, 100 mL 30 mg $\text{L}^{-1}$ $\text{KNO}_3$  | 185.59 $\mu\text{mol g}^{-1} \text{h}^{-1}$ | Chem. Eng. J., 2024, 496, 153713.          |

|  |  |  |  |
|--|--|--|--|
| ZnIn <sub>2</sub> S <sub>4</sub> -CuIn <sub>5</sub> S <sub>8</sub> | 300 W Xenon lamp, $\geq$ 400 nm, 20 mg catalyst, 100 mL 1 g L <sup>-1</sup> KNO <sub>3</sub> | 117.32<br>μmol g <sup>-1</sup> h <sup>-1</sup> | Appl. Catal. B<br>Environ, 2026,<br>383, 126110. |
|--|--|--|--|